HHS Public Access

Author manuscript

Biol Chem. Author manuscript; available in PMC 2021 July 09.

Published in final edited form as:

Biol Chem. 2019 March 26; 400(4): 501–512. doi:10.1515/hsz-2018-0280.

Interplay between reversible phosphorylation and irreversible ADP-ribosylation of eukaryotic translation elongation factor 2

Rita Mateus-Seidl,
Roche Pharma Research and Early Development, Discovery Oncology, Roche Innovation Center Munich, Nonnenwald 2, D-82377 Penzberg, FRG, Germany

Sebastian Stahl,
Roche Pharma Research and Early Development, Large Molecule Research, Roche Innovation Center Munich, Nonnenwald 2, D-82377 Penzberg, FRG, Germany

Stefan Dengl,
Roche Pharma Research and Early Development, Large Molecule Research, Roche Innovation Center Munich, Nonnenwald 2, D-82377 Penzberg, FRG, Germany

Fabian Birzele,
Roche Pharma Research and Early Development, Pharmaceutical Sciences- Bioinformatics, Roche Innovation Center Basel, Grenzacherstr. 124, CH-4070 Basel, Germany

Hedda Herrmuth,
Roche Pharma Research and Early Development, Discovery Oncology, Roche Innovation Center Munich, Nonnenwald 2, D-82377 Penzberg, FRG, Germany

Klaus Mayer,
Roche Pharma Research and Early Development, Large Molecule Research, Roche Innovation Center Munich, Nonnenwald 2, D-82377 Penzberg, FRG, Germany

Gerhard Niederfellner,
Roche Pharma Research and Early Development, Discovery Oncology, Roche Innovation Center Munich, Nonnenwald 2, D-82377 Penzberg, FRG, Germany

Xiu-Fen Liu,
Laboratory of Molecular Biology, Center for Cancer Research, National Cancer Institute, National Institutes of Health, 37 Convent Dr, Bethesda, MD 20814, USA

Ira Pastan,
Laboratory of Molecular Biology, Center for Cancer Research, National Cancer Institute, National Institutes of Health, 37 Convent Dr, Bethesda, MD 20814, USA

Ulrich Brinkmann*
Roche Pharma Research and Early Development, Large Molecule Research, Roche Innovation Center Munich, Nonnenwald 2, D-82377 Penzberg, FRG, Germany

*Corresponding author: **Ulrich Brinkmann**, ulrich.brinkmann@roche.com.

Conflict of interest statement: R.M.-S., S.S., S.D., F.B., H.H., K.M., G.N. and U.B. are employed by Roche Pharma Research & Early Development. Roche is interested in identifying novel targets and approaches for disease diagnosis and therapy.

Supplementary Material: The online version of this article offers supplementary material (https://doi.org/10.1515/hsz-2018-0280).

Abstract

The functionality of eukaryotic translation elongation factor 2 (eEF2) is modulated by phospho-rylation, eEF2 is simultaneously the molecular target of ADP-ribosylating toxins. We analyzed the interplay between phosphorylation and diphthamide-dependent ADP-ribosylation. Phosphorylation does not require diphthamide, eEF2 without it still becomes phospho-rylated. ADP-ribosylation not only modifies the H715 diphthamide but also inhibits phosphorylation of S595 located in proximity to H715, and stimulates phospho-rylation of T56. S595 can be phosphorylated by CDK2 and CDK1 which affects EEF2K-mediated T56-phosphoryla-tion. Thus, ADP-ribosylation and S595-phosphorylation by kinases occur within the same vicinity and both trig-ger T56-phosphorylation. Diphthamide is surface-acces-sible permitting access to ADP-ribosylating enzymes, the adjacent S595 side chain extends into the interior. This orientation is incompatible with phosphorylation, nei-ther allowing kinase access nor phosphate attachment. S595 phosphorylation must therefore be accompanied by structural alterations affecting the interface to ADP-ribosylating toxins. In agreement with that, replacement of S595 with Ala, Glu or Asp prevents ADP-ribosylation. Phosphorylation (starvation) as well as ADP-ribosylation (toxins) inhibit protein synthesis, both affect the S595/ H715 region of eEF2, both trigger T57-phosphorylation eliciting similar transcriptional responses. Phosphorylation is short lived while ADP-ribosylation is stable. Thus, phosphorylation of the S595/H715 ‘modifier region’ triggers transient interruption of translation while ADP-ribosylation arrests irreversibly.

Keywords

amino acid deprivation; apoptosis; diphthamide; diphtheria toxin; *Pseudomonas* exotoxin targeted therapy

Introduction

Eukaryotic elongation factor 2 (eEF2) mediates translocation of peptide-tRNA complexes from the A- to the P-site of the ribosome in a GTP-dependent manner and is essential for protein synthesis (Merrick, 1992; Kaul et al., 2011). As ‘responder’ to environmental and intracellular triggers, eEF2 plays also an important role in the regulation of protein synthesis. In particular, modifications such as T56 phosphorylation by eEF2 Kinase (eEF2K) modulate eEF2 activity and hence translation efficacy: T56 phosphorylation prevents eEF2 binding to the ribosome and thereby inhibits translation (Ovchinnikov et al., 1990; Price et al., 1991). Activation of eEF2K can be triggered by many signals. For example, AMP-dependent protein kinase (AMPK) induces eEF2K activation which leads to T56 phosphorylation in starving cells (Horman et al., 2002). EEF2 activity is also modulated by S595 phosphorylation, which in turn increases T56 phosphorylation (Hizli et al., 2013). Another position of eEF2 which is post-translationally modified is diphthamide, placed upon H715 by the concerted action of seven cellular gene products (DPH1–7) (Mattheakis et al., 1992; Nobukuni et al., 2005; Webb et al., 2008; Su et al., 2013; Dong et al., 2014; Schaffrath et al., 2014; Stahl et al., 2015b). Diphthamide serves as target of toxins including *Pseudomonas* and diphtheria toxins. Upon entering cells, these toxins bind to eEF2 in the cytoplasm and catalyze ADP-ribosylation of the diphthamide using NAD as ADP-ribosyl donor (Zhang et al., 2008). ADP-ribosylation inactivates eEF2 and thereby arrests protein

translation. The presence and composition of the H715 diphthamide is highly conserved in all eukaryotes (Van Ness et al., 1980), as well as in their archaeal counterparts. This modification may therefore also play an important role in regulation of eEF2 functionality (e.g. in translational fidelity; Liu et al., 2012), and hence in the regulation of protein synthesis.

EEF2K-mediated phosphorylation and toxin-mediated ADP-ribosylation of eEF2 both stall protein synthesis at the ribosome, but provide different initiating triggers and different outcomes for the cell. We therefore investigated if there is an interplay between eEF2 phosphorylation and ADP-ribosylation: we analyzed the influence of eEF2 phosphorylation on ADP-ribosylation and (vice versa) of ADP-ribosylation on eEF2 phosphorylation.

Results

S595 phosphorylation changes the eEF2 structure in the vicinity of the diphthamide

A model for human eEF2 in complex with *Pseudomonas* exotoxin A was created based on the structure PDB:3B82 (Joergensen et al., 2008). Human and yeast eEF2 share a sequence identity of 65.7%. Homology assignment of the human sequence on this eEF2-PE structure reveals the protein surface that interacts with PE to be identical between human and yeast, including H715 and S595. A human eEF2 structure is PDB:3J3A, a cryo-EM based model of the human 80s ribosome. In this model, human eEF2 has a different conformation than yeast eEF2 in complex with PE. The tertiary structure of the individual domains however is identical. The structure of yeast eEF2 is used as a template for the reorganization of the human eEF2 parts into a ‘PE-binding competent’ form. This is based on the assumption that the interaction mode between eEF2 and PE is mechanistically conserved. None of the amino acid changes that we implemented to humanize the yeast derived structure generated structural incompatibilities, or generated alterations in proximity to the phosphorylation sites at T56 and S595, or alterations close to H715 and its attached diphthamide. The diphthamide modification is modeled by hand. The phosphorylation site T56 is located on a loop that is not visible in the yeast structure and is thus disordered. Consequently, the loop A49-R66 was modeled and minimized by molecule typing with the CHARMM forcefield and minimizing with a conjugate gradient method including 800 steps, an root mean square (RMS) gradient of 0.1 and an energy change value of 0.0 (note: we observed a discrepancy in position designation between sequence files and literature, with T56 actually being in sequence position 57 in the sequence. For unambiguous identification, we call ‘T56’ the amino acid that is underlined in the sequence stretch AGETRFTDTR of eEF2). T56 is a substrate for phosphorylation by EEF2K, the prototype member of a protein family termed ‘alpha kinases’ because the bacterial analog of eEF2 harbors an α-helix at the position that might correspond to T56. However, neither yeast nor human structures nor secondary structure predictions indicate that T56 of eEF2 might be part of an α-helix.

The model of human eEF2 (Figure 1) reveals the eEF2K phosphorylation site T56 to be distant from S595 (>55A) and H715 diphthamide (>60A). However, S595 is close (10.4 A) to the diphthamide. The corresponding model of human eEF2 complexed with PE shows that both, S595 and H715 diphthamide are positioned in the eEF2-PE interface, i.e. in the region of complex formation between eEF2 and toxin.

S595 becomes phosphorylated by CDK-2 which modulates EEF2K mediated T56 phosphorylation. We observed that phosphoserine is structurally not tolerable at that position due to an inward-facing orientation of the S595 side chain: phospho-S595 placed into the structure generates multiple orbital overlaps of the phosphate group, e.g. with N597 and N600 of eEF2 (Figure 1C). The same incompatibilities of pS595 are observed with the original yeast eEF2-PE complex 3B82 or the human eEF2 structure 3J3A. S595 is part of a short loop which contains a proline (P596). This loop may undergo structural alterations that change the orientation of the serine and thereby may permit its phosphorylation. For example, a structurally compatible trans-cis isomerization of P596 would 'flip' the orientation of S595, making it accessible on the surface and to phosphate addition (Figure 1D). However, structural alterations as consequence of S595 phosphorylation also disturb the eEF2-PE interface, which affects complex formation between eEF2 and toxin.

The eEF2 S595 sequence can be phosphorylated by CDK1 and CDK2 and NEK2

To analyze if S595 of eEF2 can become phosphorylated not only by CDK2 (as previously described, but also by other kinases, peptides containing S595 and flanking eEF2 sequences were subjected to phosphorylation reactions with different (>200) Ser- and Thr-kinases. The results of these analyses (Figure 2) confirm phosphorylation of S595 by CDK2/CyclinB1. In addition, we observed that S595 containing peptides become also phosphorylated by CDK1/CycA, CDK1/CycB1, CDK1/CycE, and to a lesser degree by NEK2. In agreement with this observation, the eEF2 sequence flanking S595 matches consensus requirements that make S595 a substrate of CDK1 (SK**S**PNKHNR, −1K, +1P, +3K, +4H). No other CDK, and also none of the other S/T kinases caused significant phosphorylation of the peptides. This indicates that the S595 sequence of eEF2 is specifically phosphorylated by CDK1 and CDK2 and to a lesser degree by NEK2.

Diphthamide is required for ADP-ribosylation but not for phosphorylation of eEF2

MCF-7 cells and MCF7dph1ko derivatives carrying homozygous diphthamide synthesis gene *DPH1* knockouts (Stahl et al., 2015a) were analyzed to assess the influence of the H715 diphthamide on ADP-ribosylation and phosphorylation of eEF2. To analyze ADP-ribosylation, extracts containing eEF2 with (MCF-7) or without diphthamide (MCF7dph1ko) were treated with PE or DT using biotinylated NAD as substrate. ADP-ribosylated eEF2 was detected by enzyme-conjugated streptavidin which binds biotinylated ADP-ribose attached to diphthamide. Figure 3A demonstrates that eEF2 of parent MCF-7 cells becomes ADP-ribosylated by PE and DT. In contrast, eEF2 of MCF7dph1ko cells is not ADP-ribosylated. This confirms that eEF2 of homozygous DPH1 knockout cells does not carry a functional diphthamide (as a prerequisite for toxin-mediated ADP-ribosylation). To analyze if diphthamide influences serine phosphorylation of eEF2, phosphoserine-containing proteins were immunoprecipitated from extracts of MCF-7 and MCF7dph1ko cells and subsequently subjected to Western blot analyses with eEF2-specific antibodies. Figure 3B shows that pSer containing eEF2 is present to the same degree in parent MCF-7 cells as well as in MCF7dph1ko cells. This indicates that diphthamide is required for ADP-ribosylation of eEF2, but not for serine phosphorylation of eEF2. To analyze if the presence or absence of diphthamide influences T56 phosphorylation, MCF-7 and MCF7dph1ko cells were treated for 16 h with the EEF2K inducer NH125 (Chen et al., 2011). Thereafter, cell

extracts were subjected to Western blot for detection of pT56. Figure 3C shows that NH125 induces T56 phosphorylation of eEF2 to the same degree in parent and dph1ko MCF-7 which lack diphthamide. This indicates that diphthamide is not required for T56 phosphorylation.

ADP-ribosylation decreases serine phosphorylation of eEF2

To analyze if ADP ribosylation of eEF2 at H715 diphthamide influences serine phosphorylation of eEF2, we generated cell extracts of untreated MCF7 cells and of cells treated for 24 h with PE to ADP-ribosylate their eEF2. Additional samples were treated with NH125 to stimulate eEF2 phosphorylation. Phosphoserine containing proteins were subsequently immunoprecipitated followed by detection of (pS-containing) eEF2 in Western blots with eEF2 specific antibodies (Figure 4A). The results of these analyses indicated the presence of background level of S-phosphorylated eEF2 in cells that were not treated with toxins. Signals attributable to pSer containing eEF2 increased in MCF7 cells exposed to NH125. In contrast to that, decreased signals were observed in extracts of MCF7 (wildtype) cells whose eEF2 became ADP-ribosylated at H715 diphthamide due to toxin exposure. Extracts of DPH1ko cells whose eEF2 lacked diphthamide and ADP-ribosylation did not display signal reduction under the same experimental conditions. This indicates that ADP-ribosylation at H715 diphthamide reduces serine-phosphorylation of eEF2. As S595 is located adjacent to H715-diphthamide, ADP-ribosylation may directly interfere with S595 phosphorylation.

ADP-ribosylation of H715-diphthamide increases phosphorylation of T56

MCF7 extracts were subjected to Western blot analyses with antibodies that specifically detect pT56 to evaluate if ADP ribosylation influences only phosphorylation at the adjacent S595 or also at distant T56 (Figure 4). These analyses demonstrated very low levels of T56 phosphorylation in untreated controls. The EEF2K inducer NH125 increased T56 phosphorylation of eEF2. Treatment with DT or PE induced T56 phosphorylation to the same degree as exposure to NH125. Phosphorylation to even higher levels was observed upon co-administration of NH125 and PE or DT. Toxin-induced T56 phosphorylation was dependent on the presence of diphthamide, as eEF2 from DPH1 knockout cells did not show increased pT56 signals upon exposure to PE or DT. These results indicate that ADP-ribosylation stimulates T56 phosphorylation of eEF2.

Alteration of S595 interferes with toxin-mediated ADP-ribosylation

S595 phosphorylation inflicts structural alterations of eEF2 proximal to H715-diphthamide, this may affect the eEF2-toxin interface and toxin-mediated ADP-ribosylation. Because experimental determination of the influence of S595 phosphorylation is hampered by rapid dephosphorylation, eEF2 derivatives were generated that have S595 replaced with alanine, glutamate or aspartate. The latter mutations carry negative charges to mimic phosphoserine. An additional eEF2 mutant had H715 replaced by alanine. EEF2-H715A does not carry a diphthamide and therefore cannot become ADP-ribosylated. In addition to mutations, a HA-tag was placed upon the C-termini of the wildtype and mutated eEF2 derivatives to enable separation of recombinant eEF2 from cellular eEF2, and for specific detection of recombinant eEF2 derivatives. To test if ADP-ribosylation is affected, expression plasmids

encoding eEF2 and mutants were transfected into MCF7 and total cell extracts prepared 2 days later. To these extracts (containing normal cellular as well as recombinant mutated eEF2-HA), HA-binding beads and subsequently Bio-NAD and toxin were added to enable toxin-catalyzed ADP-ribosylation of HA-bound eEF2 (Figure 5A). Recombinant eEF2-HA was then separated from cellular proteins by HA affinity purification and analyzed by Western blots. Figure 5B shows that this procedure enables analyses of ADP-ribosylation of recombinant eEF2 derivatives: HA-Tag and eEF2 detecting Western blot analyses indicate successful extraction of recombinant eEF2 (positivity for eEF2 and HA antibodies at the correct size of eEF2). Detection of ADP-ribosylated eEF2 in extracts of cells transfected with HA-tagged wildtype eEF2 demonstrated that the HA-Tag does not interfere with the ADP-ribosylation reaction. Extracts of cells that were not treated with toxin, or of toxin-treated cells that contained the H715A eEF2 mutation (without diphthamide) did not generate signals for ADP-ribosylated eEF2. Thus, our assay not only shows toxin-mediated ADP-ribosylation, but also differentiates eEF2 susceptible to ADP-ribosylation from ADPR-resistant eEF2. This also proves that our preparations are not contaminated to a significant degree with cell encoded (unmutated) eEF2 as otherwise ADPR-signals would have been observed in H715A samples.

The analysis of toxin-mediated ADP-ribosylation of the different eEF2 mutants (including recombinant wildtype and H715A variants as controls) is shown in Figure 5C: signals obtained with eEF2 and HA-binding antibodies indicated that all recombinant eEF2 variants were expressed and captured by our procedure to a similar degree. ADP-ribosylated eEF2 was detected in toxin-treated extracts of cells that were transfected with wildtype eEF2-HA, but not detected in extracts of cells without toxin treatment or in toxin-treated H715A extracts. Likewise, no evidence for ADP-ribosylation of eEF2 was detectable in toxin treated extracts of cells that contained the eEF2 mutants S595A, S595D and S595E. This indicates that exchange of S595 to alanine (S595A), to glutamate (S595E) or to aspartate (S595D) interfered with ADP-ribosylation of eEF2, even though the mutated eEF2 was present in sufficient amounts (HA-tag signals) and the ADPR-reaction worked (signal positivity for HA-tagged wt eEF2). Thus, alterations at the S595 position of eEF2, including those that mimic S595 phosphorylation interfere with toxin-mediated ADP-ribosylation at H715.

ADP-ribosylation of eEF2 and amino acid deprivation induce similar transcriptional responses

EEF2K-mediated T56 phosphorylation triggers the amino acid deprivation response (Leprivier et al., 2013). Gene expression patterns of this stress response are known and appear to be very similar in different cell types (Shan et al., 2010; Kilberg et al., 2012; Balasubramanian et al., 2013). We applied genome wide Affymetrix microarray hybridizations to analyze the transcriptional response of MCF-7 cells after an exposure of 7 h to the catalytic domain of *Pseudomonas* exotoxin (PE38, Pastan et al., 2006; Hassan et al., 2016) at IC50 concentration. This truncated PE derivative without cell binding domain enters cells nonspecifically which eliminates potential signaling effects of targeted cell binding. The observed transcriptional response thereby focuses solely on consequences of the intracellular ADP-ribosylating activity of the toxin. A toxin concentration at IC_{50} (5 μm for PE38) and exposure for 7 h were chosen to allow some time for toxin uptake and

intracellular activity, yet be sufficiently early to have the cells still adherent and be able to prepare mRNA of sufficient quality. As controls, cells were exposed (7 h at IC_{50}) to toxins that kill by different mechanisms: cycloheximide (CHX, inhibits tRNA translocation and protein synthesis), α-amanitin (AMA, inhibits transcription) and geldanamycin (GA, inhibits protein folding). Principal component analyses (Figure 6A) indicated that cells respond specifically to different toxins, i.e. elicit different transcriptional responses corresponding to their different mode of action. A comparison of the individual genes that become induced upon toxin treatment reveals very little similarities in gene induction patterns between PE (protein synthesis inhibition), GA (protein folding) and Ama (RNA-Pol inhibition). Low similarities were also observed when comparing the previously observed responses to amino acid deprivation (AR) in HEPG2 cells with exposure of MCF7 to GA (protein folding) and Ama (RNA-Pol inhibition). In contrast, similar gene sets became induced in MCF7 cells exposed to the protein synthesis inhibitors PE38 and CHX, and this matched the known gene induction pattern following AR in HEPG2 (Figure 6B, C). The PE-associated mRNA profile indicated that ADP-ribosylation of eEF2 and toxin mediated protein synthesis inhibition lead to the induction of genes which represent known pathways, including ATF3, JUN, FOS, EGR network and associated factors. These stress pathways (Figure 6B, Table sT2) are also major components of transcription profiles that were previously described for the amino acid deprivation response (Supplementary Table sT2).

ADP-ribosylation is more stable than phosphorylation of eEF2

Phosphorylation of eEF2 at T56 as well as ADP-ribosylation of eEF2 at diphthamide stall protein synthesis and elicit similar transcriptional responses, yet eEF2 phosphorylation triggers pro-survival pathways, while ADP-ribosylation kills. One explanation for this may be that phosphorylation-mediated arrest of protein synthesis is reversible while ADP-ribosylation may be irreversible. To compare the stability of the modifications, cell extracts containing T56-phosphorylated eEF2 were incubated without phosphatase inhibitor at 37°C. The degree of eEF2 phosphorylation was subsequently determined after a different time of incubation by Western blot analyses. In a similar manner, eEF2 was ADP-ribosylated by PE with Bio-NAD as substrate, subsequently incubated in the presence of excess NAD (non-biotinylated to quench remaining activity of PE in the extract) without addition of any inhibitor at 37°C. The degree of ADP-ribosylation was determined after different time of incubation by detection with HRP-streptavidin as described above. The results of these analyses demonstrate that eEF2 phosphorylation is labile, with signal decreases detectable already after minutes, and complete loss of detectable eEF2 phosphorylation after 30 min (Figure 7A). In contrast, ADP-ribosylation is stable: ADP-ribosylated eEF2 was detectable without signal decrease for several hours (Figure 7B). Thus, one difference between eEF2 phosphorylation- and ADP-ribosylation mediated protein synthesis arrest and stress pathway induction is the stability of these modifications.

Discussion

The interplay between eEF2 phosphorylation and ADP-ribosylation at H715 diphthamide is summarized in Figure 8. EEF2 not phosphorylated at T56 is essential for translation elongation in protein synthesis. Temporary inhibition of this step can be tolerated by cells

but lasting inhibition is lethal. Diphthamide is conserved in eukaryotes and archaea. Nevertheless, we observed that it is neither essential for translation (diphthamide deficient cells are still viable, Supplementary S1) nor required for phosphorylation (Figure 4). EEF2K-mediated phosphorylation of T56 in response to stress situations incl. starvation inactivates eEF2 and stalls protein synthesis. EEF2 has a 'modulator region' at S595 which is a substrate for CDK2, and whose phosphorylation stimulates eEF2K-mediated T56 phosphorylation. S595 is also susceptible to phosphorylation by CDK1 (Figure 2). Interestingly, all available eEF2 structures indicate incompatibilities with S595 phosphorylation: its side chain faces into the protein preventing kinase access and leaving no space for phosphate attachment. Thus, S595 phosphorylation must be accompanied by conformational changes, possibly by a cis-trans flip of the adjacent proline 594 (Figure 1). Conformational changes may also explain that S595 phosphorylation affects eEF2K-mediated modification at the very distant positioned T56 (>55A between S595 and T56).

S595 is adjacent to H715 diphthamide (Figure 1), the target of ADP-ribosylating toxins such as DT and PE. Toxin mediated alteration of this 'modulator region' by ADP-ribosylation stimulates T56 phosphorylation (Figure 4). ADP-ribosylation of eEF2 also induces transcriptional responses and pathways that were previously described for eEF2K (i.e. T56 phosphorylation)-mediated starvation responses (Figure 6). Our data cannot differentiate between T56 phosphorylation and pathway induction being a direct consequence of ADP-ribosylation in the S595 modulator region, or a consequence of translational arrest due to ADP-ribosylation. Close proximity of S595 and H715 also explains that ADP-ribosylation at H715 (i.e. changing the environment of S595) interferes with S595 phosphorylation. Vice versa, S595 in the interface between eEF2 and toxins is important for ADP-ribosylation: alterations of S595 by mutations incl. aspartate or glutamate exchanges to mimic serine phosphorylation interfere with ADP-ribosylation of H715diphthamide (Figure 5).

Interference of eEF2 phosphorylation with toxin-mediated ADP-ribosylation may also explain observations of apparent 're-emergence' of non-modified diphthamide in cells that were previously exposed to toxins (Supplementary data S4). S595 phosphorylated eEF2 that is protected against toxin-mediated modification despite of presence of diphthamide becomes amenable to ADP-ribosylation upon dephosphorylation.

The effects of T56 phosphorylation and ADP ribosylation appear to be indistinguishable: inhibition of translational elongation and stalled protein synthesis. Also, both modifications lead to induction of similar gene sets, predominantly pro-survival pathways associated with a starvation response. A pT56 arrest that is imposed by eEF2K can be resolved by de-phosphorylation within minutes (Figure 7). This is in agreement with eEF2K mediated eEF2 inactivation serving as translational 'emergency break' under unfavorable conditions (possibly also in cell cycle stages that may not require protein synthesis). In contrast, ADP-ribosylation of eEF2 is stable with no evidence for release of this modification. This explains that ADP-ribosylation imposed by bacterial toxins can kill cells despite of the (futile) induction of pro-survival pathways.

Eukaryotic cells can counteract ADP-ribosylation and hence become resistant to bacterial toxins by various mechanisms, including restricting toxin uptake or reducing diphthamide

synthesis. Ser595 modification may be one additional way by which cells can counteract ADP-ribosylation of eEF2, because S595 phosphorylation is likely to interfere with the ADP-ribosylation reaction (Figures 1 and 5). S595 phosphorylation may have 'evolved' in eukaryotic cells not only as a measure against bacterial toxins, but possibly also to counteract ADP-ribosylation by cellular enzymes. ADP-ribosylating enzymes are activated in and drive apoptosis and it possible that that phosphorylation modulates eEF2 ADP-ribosylation at diphthamide by (so far unidentified) cellular enzymes. This 'resistance mechanism' towards ADP-ribosylating toxins/enzymes may not be relevant when sufficient ADPR-activity is present in cells. As phosphorylation is instable, ADP-ribosylation will shift the equilibrium towards irreversible eEF2 inactivation over time. On the other hand, the kinetics of ADP-ribosylation of eEF2 may be affected by S595 modification, in particular when intracellular ADP-ribosylating activity is limited.

Materials and methods

Identification of kinases that phosphorylate the S595 containing sequence of eEF2

A radiometric protein kinase assay (PanQinase Activity Assay) were applied by ProQinase GmbH (Freiburg, Germany) for measuring the kinase activity of the 229 Ser/Thr kinases; sample preparation and assay details are described in Supplementary data S2.

MCF-7 cells with homozygous knockouts of the diphthamide synthesis gene DPH1

Generation of MCF7 cells and derivatives with inactivated DPH1 genes has been previously described details are provided in the Supplementary data S1 section.

Detection of eEF2-diphthamide and of ADP-ribosylated eEF2

EEF2 with and without diphthamide was differentiated by Western blots with antibodies that either detect eEF2 irrespective of diphthamide content, or with antibodies that specifically detect eEF2 without diphthamide as described by Stahl et al. (2015b). ADP-ribosylation at H715 was analyzed in extracts of MCF7 and MCF7dph1ko cells exposed to PE and biotinylated NAD in a Western-blot like procedure, detecting ADP-ribosylated eEF2 by enzyme-conjugated streptavidin as previously described (Mayer et al., 2017): 30 μg of whole cell lysate cell lysate was incubated with 100 ng of *Pseudomonas* exotoxin A in ADP ribosylation buffer [20 mm Tris-HCl (pH 7.4), 1 mm EDTA, and 50 mm DTT] and 5 mm 6-biotin-17-NAD (Trevigen, Gaithersburg, MD, USA) in a final volume of 20 μl for 60 min at 25°C. Samples were subjected to sodium dodecyl sulfate polyacrylamide gel electrophoresis (SDS-PAGE) followed by Western blotting with streptavidin HRP conjugate (Roche, Basel, Switzerland) to detect biotin-ADP ribose-EF2. For determining the stability of ADP ribosylation of EF2, cell lysates from WT MCF7 treated overnight with toxin were kept at room temperature for 1 h, 2 h, 4 h, 6 h or 8 h before performing the ADP ribosylation assay of eEF2.

Detection of phosphorylated eEF2

Serine phosphorylation was analyzed by immunoprecipiation of phosphoserine-containing proteins from extracts of MCF-7 and MCF7dph1ko cells, followed by detecting eEF2 in the IPs by Western blots with anti-eEF2 antibodies. Phosphorylation of T56 was analyzed by

treating MCF-7 and MCF7dph1ko cells for 16 h with (or without) NH125 followed by Western blot analyses of cell extracts with an anti-phosphoT56 antibody. Therefore, sub-confluent cell cultures were lysed in RIPA buffer 50 mm Tris-HCl [(pH 7.5), 150 mm NaCl, 0.1% SDS, 0.5% sodium deoxycholate, 1% Triton X-100] supplemented with protease and phosphatase inhibitors. Total protein was quantified by the Bradford dye-binding procedure (or whatever else). Immunoprecipitation was performed by using Protein G-Agarose (Roche), according to the manufacturer's instructions. Briefly, for each sample 250 μg total lysate protein was pre-cleared with Protein G-Agarose (Roche) before incubation with 2 μg anti-phospho Serine antibody (Millipore, Burlington, MA, USA). Immunocomplexes were precipitated by addition of Protein G-Agarose and immunoprecipitated proteins were separated on SDS-PAGE. Antibodies applied bound EF-2 (H118, Santa Cruz, Dallas, TX, USA), phospho-T56 EF-2 (Cell Signaling, Leiden, the Netherlands) and Tubulin (Sigma, St. Louis, MO, USA) and were detected with Lumi-Light Western Blotting Substrate (Roche, Basel, Switzerland).

eEF2 derivatives with S595 mutations and analysis of eEF2 variants

Plasmids (pCDNA3 derivatives) for CMV-promoter driven expression encoded recombinant eEF2 and variants. Those had S595 replaced with alanine, glutamate or aspartate, or H715 replaced by alanine. A HA-tag was placed upon the C-termini of the wildtype and mutated eEF2 derivatives to enable separation of recombinant eEF2 from cellular eEF2. Expression plasmids were transfected into MCF7, total cell extracts prepared 2 days later, from which recombinant eEF2-HA was isolated by HA-binding beads. To evaluate if variants are still toxin substrates, Bio-NAD and toxin were added to enable toxin-catalyzed ADP-ribosylation of HA-bound eEF2. Recombinant eEF2-HA was then separated from cellular proteins by HA absorption and analyzed by Western blots and ADPR assays (details in Supplementary data S3).

Supplementary Material

Refer to Web version on PubMed Central for supplementary material.

Acknowledgments:

This research was supported in part by the Intramural Research Program of the NIH, National Cancer Institute, Center for Cancer Research.

References

Balasubramanian M, Shan J, and Kilberg M (2013). Dynamic changes in genomic histone association and modification during activation of the *ASNS* and *ATF3* genes by amino acid limitation. Biochem. J. 449, 219. [PubMed: 22978410]

Chen Z, Gopalakrishnan SM, Bui MH, Soni NB, Warrior U, Johnson EF, Donnelly JB, and Glaser KB (2011). 1-Benzyl-3-cetyl-2-methylimidazolium iodide (NH125) induces phosphorylation of eukaryotic elongation factor-2 (eEF2): a cautionary note on the anticancer mechanism of an eEF2 kinase inhibitor. J. Biol. Chem. 286, 43951–43958. [PubMed: 22020937]

Dong M, Su X, Dzikovski B, Dando EE, Zhu X, Du J, Freed JH, and Lin H (2014). Dph3 Is an electron donor for Dph1-Dph2 in the first step of eukaryotic diphthamide biosynthesis. J. Am. Chem. Soc. 136, 1754–1757. [PubMed: 24422557]

Hassan R, Alewine C, and Pastan I (2016). New life for immunotoxin cancer therapy. Clin. Cancer Res. 22, 1055. [PubMed: 26463707]

Hizli AA, Chi Y, Swanger J, Carter JH, Liao Y, Welcker M, Ryazanov AG, and Clurman BE (2013). Phosphorylation of eukaryotic elongation factor 2 (eEF2) by cyclin A-cyclin-dependent kinase 2 regulates its inhibition by eEF2 kinase. Mol. Cell. Biol. 33, 596. [PubMed: 23184662]

Horman S, Browne GJ, Krause U, Patel JV, Vertommen D, Bertrand L, Lavoinne A, Hue L, Proud CG, and Rider MH (2002). Activation of AMP-activated protein kinase leads to the phosphorylation of elongation factor 2 and an inhibition of protein synthesis. Curr. Biol. 12, 1419–1423. [PubMed: 12194824]

Hu X, Wei H, Xiang L, Chertov O, Wayne AS, Bera TK, and Pastan I (2013). Methylation of the DPH1 promoter causes immunotoxin resistance in acute lymphoblastic leukemia cell line KOPN-8. Leukemia Res. 37, 1551–1556. [PubMed: 24070652]

Joergensen R, Wang Y, Visschedyk D, and Merrill AR (2008). The nature and character of the transition state for the ADP-ribosyltransferase reaction. EMBO Rep. 9, 802–809. [PubMed: 18583986]

Kaul G, Pattan G, and Rafeequi T (2011). Eukaryotic elongation factor-2 (eEF2): its regulation and peptide chain elongation. Cell Biochem. Funct. 29, 227–234. [PubMed: 21394738]

Kilberg MS, Balasubramanian M, Fu L, and Shan J (2012). The transcription factor network associated with the amino acid response in mammalian cells. Adv. Nutr. 3, 295–306. [PubMed: 22585903]

Leprivier G, Remke M, Rotblat B, Dubuc A, Mateo AR, Kool M, Agnihotri S, El-Naggar A, Yu B, Prakash-áSomasekharan S, et al. (2013). The eEF2 kinase confers resistance to nutrient deprivation by blocking translation elongation. Cell 153, 1064–1079. [PubMed: 23706743]

Liu S, Bachran C, Gupta P, Miller-Randolph S, Wang H, Crown D, Zhang Y, Wein AN, Singh R, Fattah R, et al. (2012). Diphthamide modification on eukaryotic elongation factor 2 is needed to assure fidelity of mRNA translation and mouse development. Proc. Natl. Acad. Sci. USA 109, 13817. [PubMed: 22869748]

Mattheakis LC, Shen WH, and Collier RJ (1992). DPH5, a methyltransferase gene required for diphthamide biosynthesis in *Saccharomyces cerevisiae*. Mol. Cell. Biol. 12, 4026. [PubMed: 1508200]

Mayer K, Schroeder A, Schnitger J, Stahl S, and Brinkmann U (2017). Influence of DPH1 and DPH5 protein variants on the synthesis of diphthamide, the target of ADPRibosylating toxins. Toxins 9, 78.

Merrick WC (1992). Mechanism and regulation of eukaryotic protein synthesis. Microbiol. Rev. 56, 291–315. [PubMed: 1620067]

Nobukuni Y, Kohno K, and Miyagawa K (2005). Gene trap mutagenesis-based forward genetic approach reveals that the tumor suppressor OVCA1 is a component of the biosynthetic pathway of diphthamide on elongation factor 2. J. Biol. Chem. 280, 10572–10577. [PubMed: 15637051]

Ovchinnikov LP, Motuz LP, Natapov PG, Averbuch LJ, Wettenhall REH, Szyszka R, Kramer G, and Hardesty B (1990). Three phosphorylation sites in elongation factor 2. FEBS Lett. 275, 209–212. [PubMed: 2261989]

Pasetto M, Antignani A, Ormanoglu P, Buehler E, Guha R, Pastan I, Martin SE, and FitzGerald DJ (2015). Whole-genome RNAi screen highlights components of the endoplasmic reticulum/Golgi as a source of resistance to immunotoxin-mediated cytotoxicity. Proc. Natl. Acad. Sci. USA 112, E1135. [PubMed: 25713356]

Pastan I, Hassan R, FitzGerald DJ, and Kreitman RJ (2006). Immunotoxin therapy of cancer. Nat. Rev. Cancer 6, 559. [PubMed: 16794638]

Price NT, Redpath NT, Severinov KV, Campbell DG, Russell JM, and Proud CG (1991). Identification of the phosphorylation sites in elongation factor-2 from rabbit reticulocytes. FEBS Lett. 282, 253–258. [PubMed: 2037042]

Schaffrath R, bdel-Fattah W, Klassen R, and Stark MJR (2014). The diphthamide modification pathway from *Saccharomyces cerevisiae* revisited. Mol. Microbiol. 94, 1213–1226. [PubMed: 25352115]

Shan J, Lopez MC, Baker HV, and Kilberg MS (2010). Expression profiling after activation of amino acid deprivation response in HepG2 human hepatoma cells. Physiol. Genomics 41, 315–327. [PubMed: 20215415]

Stahl S, Mueller F, Pastan I, and Brinkmann U (2015a). Factors that determine sensitivity and resistances of tumor cells towards antibody-targeted protein toxins. In: Resistance to Immunotoxins in Cancer Therapy. Resistance to Targeted Anti-Cancer Therapeutics, Verma R and Bonavida B, eds. (Cham, Switzerland: Springer).

Stahl S, da Silva Mateus Seidl AR, Ducret A, Kux van Geijtenbeek S, Michel S, Racek T, Birzele F, Haas AK, Rueger R, Gerg M, et al. (2015b). Loss of diphthamide preactivates NFkB and death receptor pathways and renders MCF7 cells hypersensitive to tumor necrosis factor. Proc. Natl. Acad. Sci. USA 112, 10732. [PubMed: 26261303]

Su X, Lin Z, and Lin H (2013). The biosynthesis and biological function of diphthamide. Crit. Rev. Biochem. Mol. Biol. 48, 515–521. [PubMed: 23971743]

Van Ness BG, Howard JB, and Bodley JW (1980). ADP-ribosylation of elongation factor 2 by diphtheria toxin. Isolation and properties of the novel ribosyl-amino acid and its hydrolysis products. J. Biol. Chem. 255, 10717–10720. [PubMed: 7000782]

Webb TR, Cross SH, McKie L, Edgar R, Vizor L, Harrison J, Peters J, and Jackson IJ (2008). Diphthamide modification of eEF2 requires a J-domain protein and is essential for normal development. J. Cell Sci. 121, 3140. [PubMed: 18765564]

Wei H, Xiang L, Wayne AS, Chertov O, FitzGerald DJ, Bera TK, and Pastan I (2012). Immunotoxin resistance via reversible methylation of the DPH4 promoter is a unique survival strategy. Proc. Natl. Acad. Sci. USA 109, 6898. [PubMed: 22509046]

Wei H, Bera TK, Wayne AS, Xiang L, Colantonio S, Chertov O, and Pastan I (2013). A modified form of diphthamide causes immunotoxin resistance in a lymphoma cell line with a deletion of the *WDR85* gene. J. Biol. Chem. 288, 12305–12312. [PubMed: 23486472]

Zhang Y, Liu S, Lajoie G, and Merrill A (2008). The role of the diphthamide-containing loop within eukaryotic elongation factor 2 in ADP-ribosylation by *Pseudomonas aeruginosa* exotoxin A. Biochem. J. 413, 163. [PubMed: 18373493]

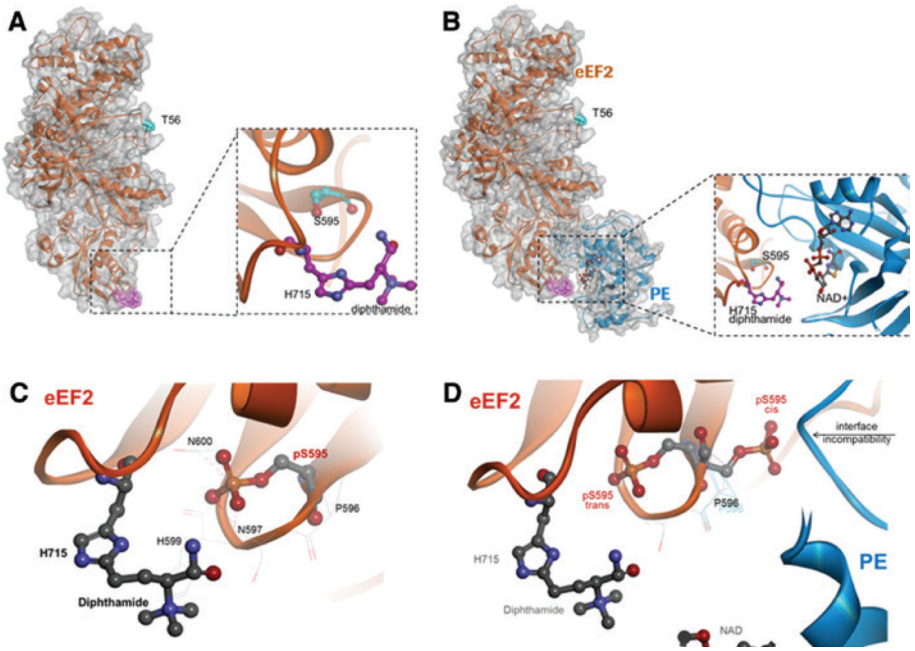

Figure 1:

Structure model of human eEF2.

(A) The model was generated by humanizing the X-ray structure PDB:3B82 (complex of *Saccharomyces cerevisiae* eEF2, PE and NAD+). None of the amino acid changes implemented to humanize generated structural incompatibilities in proximity to the phosphorylation sites at T56 and S595, or close to H715 and diphthamide. We observed a discrepancy in position designation between sequence files and literature with T56 actually being position 57 in the sequence. For unambiguous identification, we call T56 the amino acid that is underlined in the sequence stretch AGETRFTDTR of eEF2. (B) Human eEF2 complex with *Pseudomonas* exotoxin A. PDB:3B82 was humanized as described in (A). The protein surface that interacts with PE is identical between human and yeast. (C) Phosphorylation of S595 is incompatible with the human eEF2 model and other eEF2 structures. S595 faces inwards and is therefore not accessible to kinases. An attached phosphate would clash with N597 and N600. (D) Trans to cis isomerization of P596 ‘flips’ the S595 containing loop and thereby directs S595 to the surface of eEF2. The flip was modeled by superimposing a cis-trans peptide ‘Gly-Pro’ from the structure 4ICB, subsequently placing pS according to the cis-pep coordinates. This alters the orientation of S595 but not the remainder of the structure. In this orientation, S595 would be accessible to kinases and phosphorylation is structurally compatible. However, cis-pS595 extends into and hence disturbs the interface of eEF2 and PE.

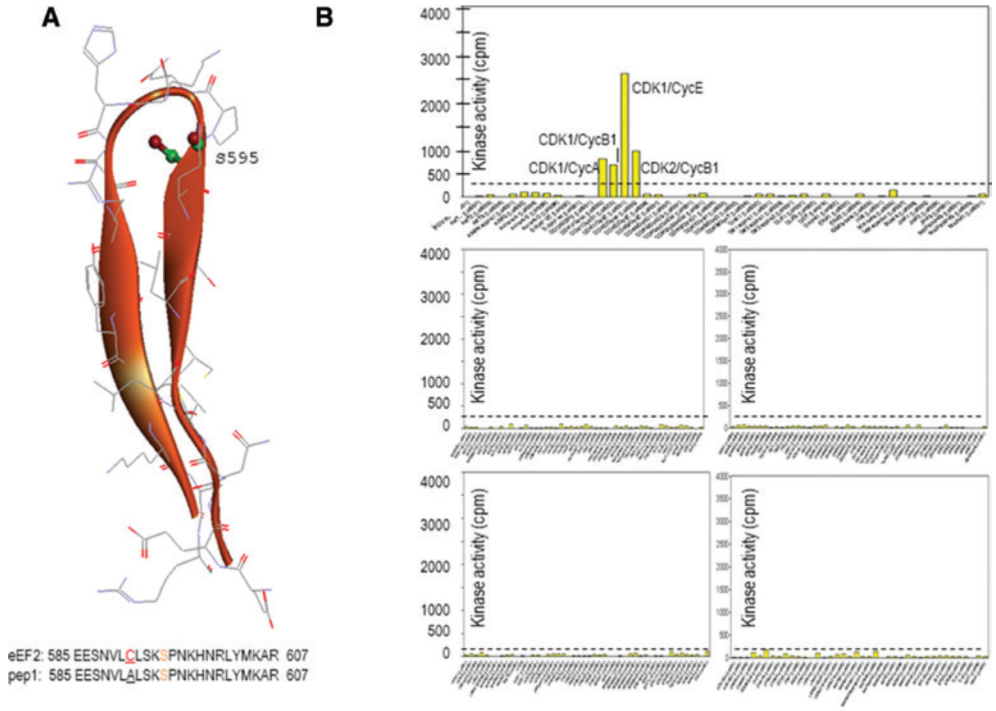

Figure 2:

Phosphorylation of S595 containing peptides by CDK1, CDK2 and NEK2.

(A) Peptides that comprise the S595 region are displayed in the structural context of eEF2. Pep1 is linear, pep2 and 3 constrained by disulfides to support a loop. (B) To identify S/T kinases that phosphorylate the peptides, a kinase screen encompassing phosphorylation assays with all three peptides on 200 known S/T kinases was performed (ProQinase screen, details in Supplementary Data S2). As reaction buffers contained reducing agents, peptides may have become linearized in those assays. Signals above background were observed only for CDK1, CDK2 and NEK2 but not for any other kinase (shown exemplarily for peptide 2, complete data set in Supplementary Data S2).

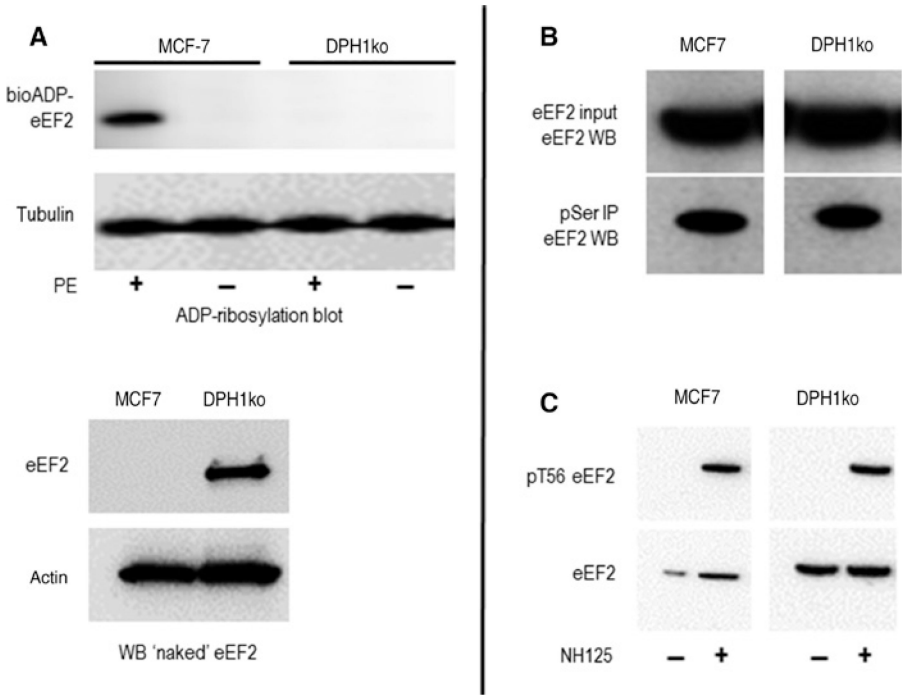

Figure 3:

Diphthamide is necessary for eEF2 ADP-ribosylation but not phosphorylation.

(A) Upper panel: ADP-ribosylation at H715 was analyzed in extracts of MCF7 and MCF7dph1ko cells exposed to PE and biotinylated NAD. ADP-ribosylated eEF2 was detected by enzyme-conjugated streptavidin which binds bio-ADP-ribose attached to eEF2. EEF2 of parent MCF-7 becomes ADP-ribosylated but eEF2 of MCF7dph1ko cells is not ADP-ribosylated due to lack of diphthamide. Lower panel: DPH1ko cells harbor eEF2 without diphthamide and hence can be detected by an antibody that specifically binds eEF2 without diphthamide. (B) Serine phosphorylation was analyzed by immunoprecipiation (IP) of phosphoserine-containing proteins from extracts of MCF-7 and MCF7dph1ko cells, followed by detecting eEF2 in the IPs by Western Blots with anti-eEF2 antibodies. (C) Phosphorylation of T56 was analyzed by treating MCF-7 and MCF7dph1ko cells for 16h with NH125 (19) followed by Western blot analyses of cell extracts with an anti-phosphoT56 antibody. Comparison of MCF7 and MCF7dph1ko cells reveals no difference in pSer or NH125 induced T56 phosphorylation. Thus, diphthamide is not required for eEF2 phosphorylation.

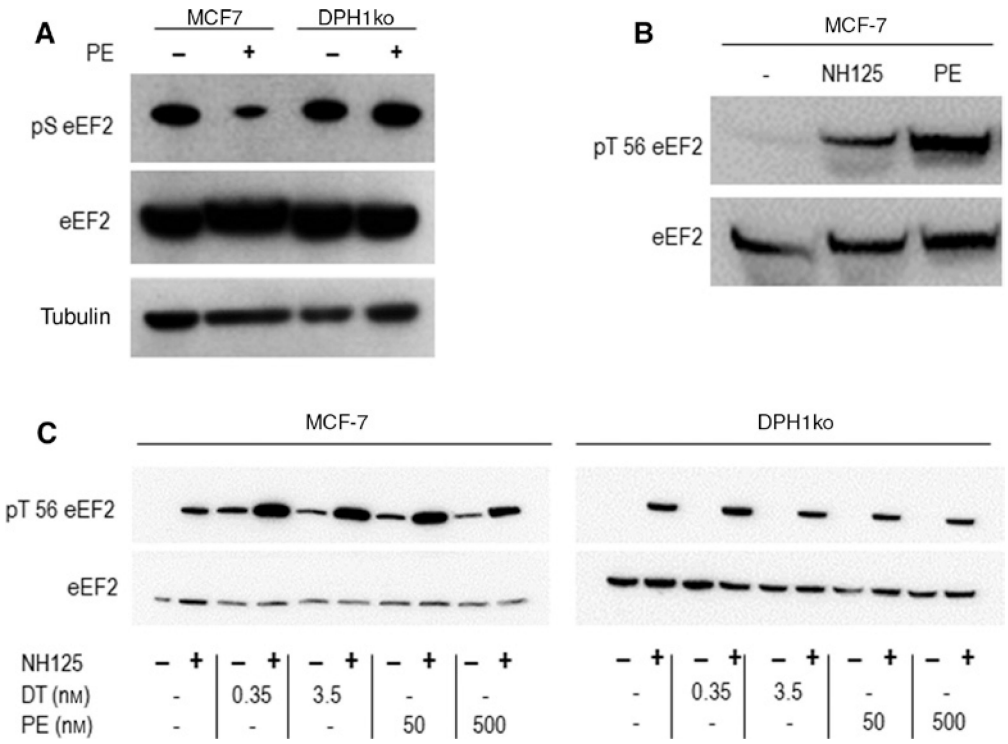

Figure 4:

ADP-ribosylation decreases serine phosphorylation and increases threonine-56 phosphorylation.

(A) Serine phosphorylation: Diphthamide-containing MCF-7 cells exposed to PE contain ADP-ribosylated H715 in close proximity to S595. This reduces phosophoserine-eEF2 signals (pS eEF2-assay as described in Figure 3). Phosphoserine-eEF2 signals did not decrease in toxin-treated DPH1ko cells. (B and C) T56 phosphorylation: Western blot analyses (pT56eEF2-assay as described in Figure 3) detect pT56 upon treatment of MCF-7 with NH125. T56 phosphorylation is also induced by treatment with ADP-ribosylating toxins PE and DT. DPH1ko cells did not induce T56 phosphorylation upon toxin exposure but phosphorylated T56 in response to NH125.

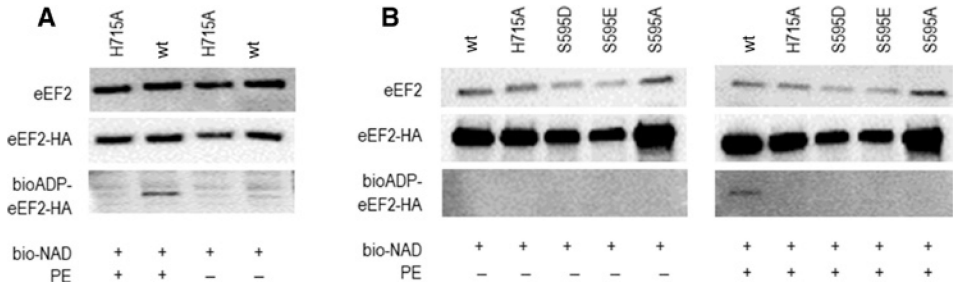

Figure 5:

S595 alteration affects ADP-ribosylation of eEF2.

(A) EEF2 containing a HA-tag was expressed in MCF7 cells, subsequently captured on beads, exposed to toxin and Bio-NAD and thereafter separated from cellular eEF2 via isolation of the (magnetic) beads and analyzed by Western blots to evaluate ADP-ribosylation. Anti-eEF2 and anti-HA blots demonstrate presence of recombinant eEF2 in all samples, but only wildtype eEF2 becomes ADP-ribosylated upon toxin exposure. The H715A mutated eEF2 does not show signals associated with ADP-ribosylation as it lacks diphthamide. (B) Analyses of S595 mutants show that altering S595 by replacing it with alanine, glutamate or aspartate interferes with toxin-mediated ADP ribosylation.

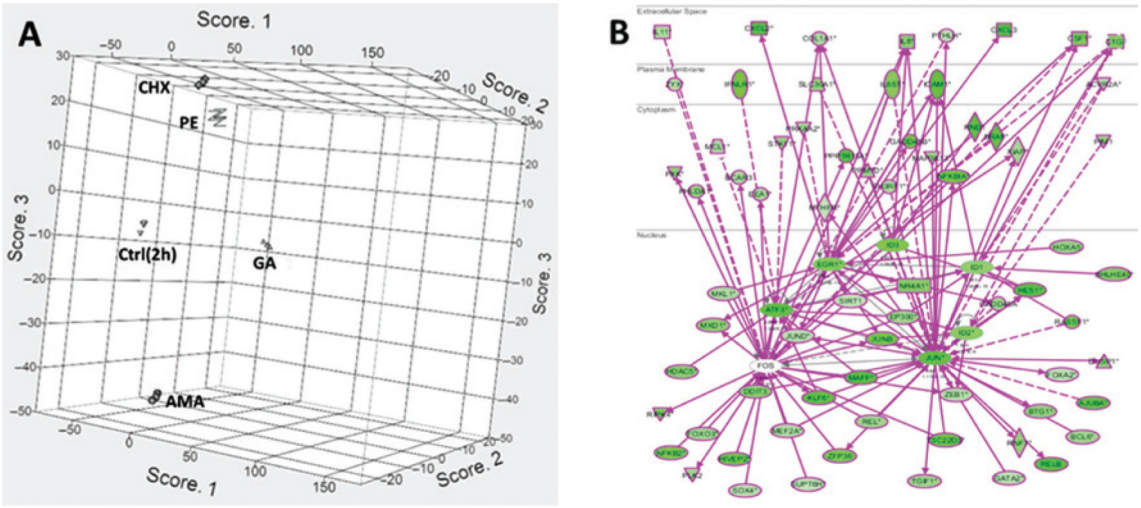

C

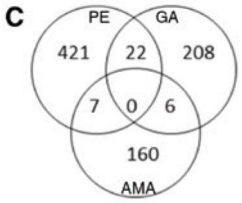

Treatment	Total	Shared	% of total	% of PE	% of GA	% of AMA
PE + GA + AMA	824	0	0	0	0	0
PE + GA	651	22	3	5	9	-
PE + AMA	610	7	1	2	-	4
GA + AMA	403	6	2	-	3	8

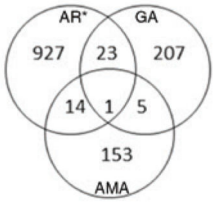

Treatment	Total	Shared	% of total	% of AR	% of GA	% of AMA
AR + GA + AMA	1325	1	0	0	0	1
AR + GA	1172	24	2	2	10	-
AR + AMA	1118	15	1	2	-	9
GA + AMA	403	6	2	-	3	8

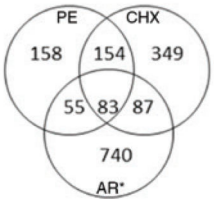

Treatment	Total	Shared	% of total	% of PE	% of CHX	% of AR
PE + CHX + AR	1662	83	5	18	12	9
PE + CHX	886	237	27	53	35	-
PE + AR	1313	138	10	30	-	14
AR + CHX	1504	170	11	-	25	18

Figure 6:

ADP-ribosylation of eEF2 induces starvation response pathway genes.

(A) Principal component analysis of transcriptional responses of MCF-7 exposed for 7 h to IC_{50} concentration of truncated *Pseudomonas* exotoxin (PE), geldanamycin (GA), cycloheximide (CHX) or α-amanitin (AMA). Clear differentiation of the responses is indicated for toxins with different mode of action. PE and CHX which both inhibit translation appear similar. (B) Exposure of MCF-7 to PE induces a transcriptional response and pathways similar to those observed in amino acid restriction responses. The ingenuity plot summarizes pathway relations of the genes that are induced by PE in MCF-7, as well as in HepG2 upon amino acid deprivation (see Supplementary Table sT2 for a complete list). (C) Genes that are induced 7 h after exposure of MCF7 cells to IC_{50} concentrations of truncated *Pseudomonas* exotoxin (PE), geldanamycin (GA), cycloheximide (CHX) or α-

amanitin (AMA). AR* is a gene set which is upregulated in starved HepG2 cells (21). Note the dissimilarity between PE vs. GA and Ama in MCF-7, and the similarity between the protein synthesis inhibitors PE and CHX with A.

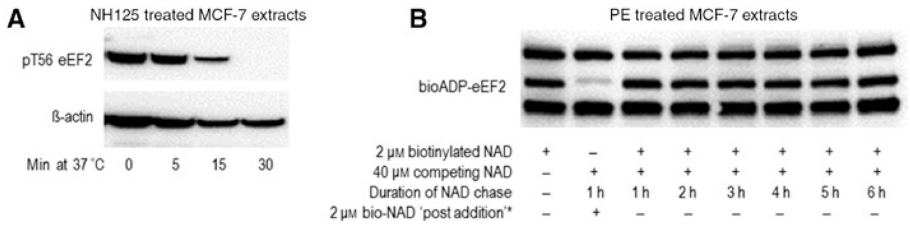

Figure 7:

Phosphorylation of eEF2 is instable while ADP-ribosylation is stable.

(A) MCF7 cells were treated with NH125 to stimulate NT56 phosphorylation. Extracts without phosphatase inhibitors were kept for the indicated time at 37°C. Detection of pT56 eEF2 demonstrates that eEF2 de-phosphorylates within minutes. (B) MCF7 cell extracts were treated with PE and Bio-NAD and subsequently subjected to a chase with non-biotinylated NAD and incubated for the indicated time at 37°C. (*) Chase with 20-fold excess non-labeled NAD blocks toxin-mediated incorporation of bio-NAD as shown in the sample which received non-labeled NAD first followed by bio-NAD 1 h later. ADP-ribosylation followed by NAD-chase and detection of Bio-ADP coupled to eEF2 demonstrates that ADP-ribosylation of eEF2 remains stable for hours.

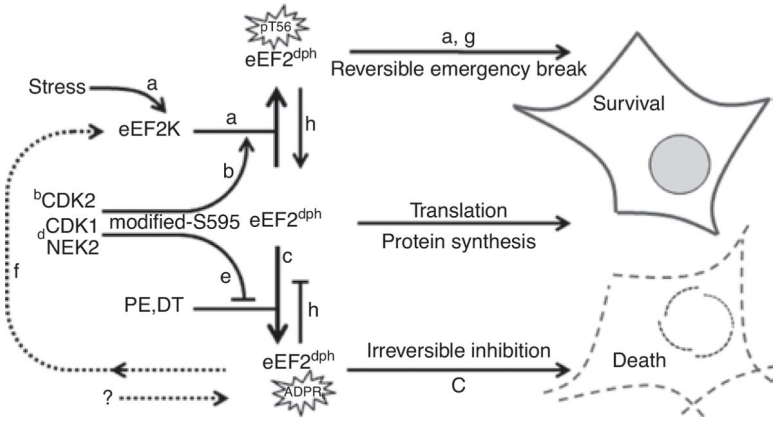

Figure 8:

Interplay between phosphorylation and ADP-ribosylation of eEF2.

(a) The interaction scheme bases on previously described responses to eEF2K-mediated T56 phosphorylation (1–5), (b) CDK2-mediated S595 phosphorylation (6) and (c) toxin-mediated H715 ADP-ribosylation (7–9, 17, 18, 24–29). We added results from the kinase screen (d, Figure 2), S595 mutagenesis (e, Figure 5), ADP-ribosylation and phosphorylation analyses (f, Figure 4), transcriptional profiling (g, Figure 6), and stability experiments (h, Figure 7) in MCF7 cells (Wei et al., 2012, 2013; Hu et al., 2013; Pasetto et al., 2015).